# RESEARCH NOTE

# MATHEMATICAL MODELING OF POTENTIAL FLOW OVER A ROTATING CYLINDER

***S. Askari*, M. H. Shojaeefard***

*Department of Mechanical Engineering, Iran University of Science and Technology, Narmak, Tehran 16844, Iran*
*bas_salaraskari@yahoo.com*

*Corresponding Author

**(Received: March 1, 2009 – Accepted in Revised Form: March 11, 2010)**

**Abstract** Potential flow over rotating cylinder is usually solved by the singularity method. However, in this paper a mathematical solution is presented for this problem by direct solution of the Laplace's equation. Flow over the cylinder was considered non-viscous. Neumann and Dirichlet boundary conditions were used on the solid surfaces and in the infinity, respectively. Because of non-viscous flow, the Laplace equation is the governing equation of the flow field. The entire flow field was divided into two parts including free stream over a stationary cylinder and flow over a rotating cylinder with no free stream. Because of linearity of the governing equation, solutions of these flows were superposed to obtain velocity potential function from which velocity and pressure distribution was obtained. Pressure forces acting on the cylinder were obtained by integrating pressure distribution over the cylinder surface that was exactly the same as the results of the singularity method. Present work achieved the famous Kutta-Joukowski theorem in the aerodynamics and fluid mechanics. In addition, the proposed analytical model was validated by numerical solution.

**Keywords** Bernoulli equation, Laplace equation, Potential flow, Kutta-Joukowski theorem, Singularity method, CFD, Finite Volume Method (FVM)

**چکیده** جریان پتانسیل پیرامون استوانه چرخان معمولا با روش سینگولاریتی حل می شود. اما در این مقاله یک حل ریاضی با استفاده از حل معادله لاپلاس برای این مساله ارایه شده است. جریان پیرامون استوانه غیر ویسکوز در نظر گرفته شده و شرایط مرزی نیومان و دیریکله به ترتیب برای سرعت روی سطوح جامد و پتانسیل سرعت در بی نهایت بکار رفته است. مساله به دو قسمت شامل جریان آزاد پیرامون استوانه بدون دوران و جریان پیرامون استوانه دوار بدون جریان آزاد تقسیم شد. به دلیل خطی بودن معادله حاکم، این دو جواب برهم نهی شدند تا جواب کامل مساله بدست آید. توزیع سرعت و فشار با استفاده از تابع پتانسیل سرعت بدست آمد. نیروهای فشاری وارد بر استوانه با انتگرالگیری توزیع فشار محاسبه شدند که دقیقا با نتایج روش سینگولاریتی یکسان بودند. در این مقاله قضیه معروف کاتا- جاکوفسکی در آیرودینامیک و مکانیک سیالات با روش ریاضی بدست آمده است. علاوه بر این، حل تحلیلی با نتایج حل عددی مقایسه شد که صحت آن مورد تایید قرار گرفت.

## 1. INTRODUCTION

Flow over stationary and rotating cylinders is of high interest in industry and theoretical fluid mechanics and aerodynamics. In 1924, Flettner used a couple of rotating cylinders to produce propulsive force for his famous ship [1]. Recently, Peebles has invented a new airplane called FanWing that utilizes a mechanism as in rotating cylinder for generating lift force. In his innovative model, a cross flow fan plays role of the rotating cylinder [2-7]. Mirzaee, et al [8] studied flow over a cylinder by Finite Volume Method (FVM) that was consistent with the available experimental and numerical data. Lopez, et al [9] investigated instability and mode interactions in a differentially driven rotating cylinder by solving Navier-Stokes equations and experimental measurements. Rahimi calculated pressure in the flow between two eccentric rotating cylinders by using perturbation method [10]. Heidarinejad and Delfani surveyed the wake flow behind a cylinder using random vortex method. They showed that variation of geometrical and physical parameters of the flow strongly depends on the Reynolds number [11].

Objective of this work is to present a mathematical

model for the potential flow over a rotating cylinder by exact solution of the Laplace equation. Traditionally, in aerodynamics and fluid mechanics, flow over the rotating cylinder is solved by superposition of a doublet, an irrotational vortex and a free stream [1,12,13]. Doublet and irrotational vortex are artificial singularities not existing in reality. Because some concepts like vortex and doublet strength are physically ambiguous, the approach presented in this paper is more understandable than singularity method. For example, the angular velocity of the rotating cylinder is more tangible than the strength of a vortex.

## 2. ANALYTICAL SOLUTION

Flow over a rotating cylinder is shown in Figure 1. It can be decomposed into two flows, a rotating cylinder with no free stream and a stationary cylinder with a free stream.

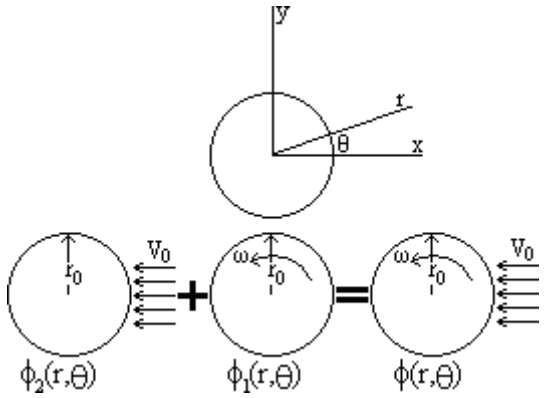


**Figure 1.** Potential flow over a rotating cylinder

The governing equation of the flow field is linear and velocity potential is obtained from superposition of solutions of these subproblems.

$$\phi(r,\theta)=\phi_1(r,\theta)+\phi_2(r,\theta)$$

One of the basic boundary conditions for potential flows is that component of the velocity vector normal to any solid surface in the flow field should be zero. Velocity of the flow at the surface of the cylinder is equal to the tangential component of the velocity vector and consequently boundary conditions for $\phi_1(r,\theta)$ are as

$$\begin{cases} u_r=\left(\dfrac{\partial\phi_1}{\partial r}\right)_{r=r_0}=0 \\ \qquad\qquad\qquad\qquad \Rightarrow \phi_1(r,\theta)=r_0^2\omega\theta \\ u_\theta=\left(\dfrac{1}{r}\dfrac{\partial\phi_1}{\partial\theta}\right)_{r=r_0}=r_0\omega \end{cases}$$

Free stream velocity is $V_0$ and its velocity potential is as followings [1,12,13]

$$\phi_0(x,y)=-V_0x$$

It can be written in polar coordinates system as

$$\phi_0(r,\theta)=-V_0r\cos\theta \qquad (1)$$

Laplace equation and its boundary conditions for these problem are given as followings [1,12,13]

$$\begin{aligned} &\frac{\partial^2\phi_2}{\partial r^2}+\frac{1}{r}\frac{\partial\phi_2}{\partial r}+\frac{1}{r^2}\frac{\partial^2\phi_2}{\partial\theta^2}=0 \\ &\text{(a)}\quad \lim_{r\to\infty}\phi_2(r,\theta)=-V_0r\cos\theta \\ &\text{(b)}\quad \frac{\partial\phi_2(r=r_0,\theta)}{\partial r}=0,\ 0\le\theta\le 2\pi \end{aligned} \qquad (2)$$

Equation 2 describes a Neumann problem over a disk of radius $r_0$ with a Dirichlet condition at infinity. Using the separation of variables method, solution of Equation 2 is considered as [14,15]

$$\phi_2(r,\theta)=R(r)\Theta(\theta) \qquad (3)$$

Plugging Equation 3 into Equation 2, results in

$$r^2R''\Theta+rR'\Theta+R\Theta''=0\Rightarrow\frac{r^2R''+rR'}{R}+\frac{\Theta''}{\Theta}=0\Rightarrow\frac{r^2R''+rR'}{R}=-\frac{\Theta''}{\Theta}=k\Rightarrow$$
$$r^2R''+rR'-kR=0 \text{ and } \Theta''+k\Theta=0$$

It is obvious that velocity potential should be a $2\pi$-periodic function of $\theta$ as $\phi_2(r,\theta)=\phi_2(r,\theta+2\pi)$ and consequently k must be a positive integer as $k=n^2$.

$$\Theta_n(\theta) = a_n \cos n\theta + b_n \sin n\theta,\ n = 0, 1, \ldots \quad (4)$$

Equation $r^2R''+rR'-kR=0$ is known as the Euler equation and its characteristic equation is given by [14,16]

$$\xi^2 + (1-1)\xi - n^2 = 0 \Rightarrow \xi_1 = n,\quad \xi_2 = -n$$

Thus, R is as followings [14,16]

$$\text{(i).If } n \neq 0 : R(r) = C_1\left(\frac{r}{r_0}\right)^n + C_2\left(\frac{r}{r_0}\right)^{-n}$$

$$\text{(ii).If } n = 0 : R(r) = C_3 + C_4 \ln\left(\frac{r}{r_0}\right)$$

R is equal to sum of the above solutions

$$R_n(r) = C_1(\frac{r}{r_0})^n + C_2(\frac{r}{r_0})^{-n} + C_3 + C_4 \ln(\frac{r}{r_0}) \quad (5)$$

Using Equations 3, 4 and 5, Eigenfunctions of the Laplace equation are as

$$\phi_{2,n}(r,\theta) = \left(C_1(\frac{r}{r_0})^n + C_2(\frac{r}{r_0})^{-n} + C_3 + C_4 \ln(\frac{r}{r_0})\right) \times \left(a_n \cos n\theta + b_n \sin n\theta\right) \quad (6)$$

Superposing these Eigenfunctions yields

$$\phi_2(r,\theta) = \sum_{n=1}^{n=\infty}\left(C_1(\frac{r}{r_0})^n + C_2(\frac{r}{r_0})^{-n} + C_3 + C_4 \ln(\frac{r}{r_0})\right) \times \left(a_n \cos n\theta + b_n \sin n\theta\right) \quad (7)$$

Where $C_1$, $C_2$, $C_3$, $C_4$, $a_n$ and $b_n$ can be obtained by applying Neumann and Dirichlet boundary conditions given in Equation 2.

Applying the first boundary condition, Equation 2(a), on Equation 7 gives

$$\lim_{r\to\infty} \phi_2(r,\theta) = \lim_{\substack{n=1 \\ r\to\infty}}^{n=\infty}\left(C_1(\frac{r}{r_0})^n + C_2(\frac{r}{r_0})^{-n} + C_3 + C_4 \ln(\frac{r}{r_0})\right) \times \left(a_n \cos n\theta + b_n \sin n\theta\right) =$$

$$\sum_{n=1}^{n=\infty}\left(C_1(\frac{r}{r_0})^n + C_3 + C_4 \ln(\frac{r}{r_0})\right) \times \left(a_n \cos n\theta + b_n \sin n\theta\right) = -V_0 r\cos\theta \Rightarrow$$

$$n = 1, C_4 = 0, C_3 = 0$$

$$\left(a_1 \cos\theta + b_1 \sin\theta\right) C_1 \frac{r}{r_0} = -V_0 r\cos\theta \Rightarrow$$

$$a_1 C_1 = -V_0 r,\ b_1 C_1 = 0$$

The first order partial derivative of the velocity potential function with respect to r is

$$\frac{\partial\phi_2(r,\theta)}{\partial r} = \sum_{n=1}^{n=\infty}\left(C_1 \frac{n}{r_0}(\frac{r}{r_0})^{n-1} - C_2 \frac{n}{r_0}(\frac{r}{r_0})^{-n-1} + C_4 \frac{r}{r_0}\right) \times \left(a_n \cos n\theta + b_n \sin n\theta\right)$$

Using the second boundary condition, Equation 2(b), and above equation yields

$$n(C_1 - C_2) + C_4 = 0, n = 1, C_4 = 0 \Rightarrow C_1 = C_2 \Rightarrow$$

$$\phi(r,\theta) = \left(C_1(\frac{r}{r_0})^1 + C_2(\frac{r}{r_0})^{-1}\right)\left(a_1 \cos\theta + b_1 \sin\theta\right)$$

$$= \left(\frac{r}{r_0} + \frac{r_0}{r}\right)\left(C_1 a_1 \cos\theta + C_1 b_1 \sin\theta\right) =$$

$$\left(\frac{r}{r_0} + \frac{r_0}{r}\right)(-V_0 r_0 \cos\theta) \Rightarrow$$

$$\phi_2(r,\theta) = -V_0\left(r + \frac{r_0^2}{r}\right)\cos\theta \Rightarrow$$

$$\phi(r,\theta) = -V_0\left(r + \frac{r_0^2}{r}\right)\cos\theta + r_0^2\omega\theta \quad (8)$$

According to the definition of the stream function it can be obtained as followings [1,12,13]

$$u_r = \frac{1}{r}\frac{\partial \varphi}{\partial \theta} = -V_0\left(1-\frac{r_0^2}{r^2}\right)\cos\theta \Rightarrow$$

$$\frac{\partial \varphi}{\partial \theta} = -V_0\left(r-\frac{r_0^2}{r}\right)\cos\theta$$

$$\Rightarrow \varphi(r,\theta) = -V_0\left(r-\frac{r_0^2}{r}\right)\sin\theta + f(r)$$

$$u_\theta = -\frac{\partial \varphi}{\partial r} = V_0\left(1+\frac{r_0^2}{r^2}\right)\sin\theta + \frac{r_0^2\omega}{r} =$$

$$V_0\left(1+\frac{r_0^2}{r^2}\right)\sin\theta - \frac{df}{dr} \Rightarrow \frac{df}{dr} = -\frac{r_0^2\omega}{r} \Rightarrow$$

$$f(r) = -r_0^2\omega\ln r \Rightarrow$$

$$\varphi(r,\theta) = -V_0\left(r-\frac{r_0^2}{r}\right)\sin\theta - r_0^2\omega\ln r \qquad (9)$$

## 3. STAGNATION POINTS

Components of the velocity vector are as below [1,12,13]

$$u_r = \frac{\partial \phi}{\partial r} = -V_0\left(1-\frac{r_0^2}{r^2}\right)\cos\theta$$

$$u_\theta = \frac{1}{r}\frac{\partial \phi}{\partial \theta} = V_0\left(1+\frac{r_0^2}{r^2}\right)\sin\theta + \frac{r_0^2\omega}{r}$$

By definition, velocity components are zero at stagnation point [1,12,13]. Thus,

$$V_0\left(1+\frac{r_0^2}{r^2}\right)\sin\theta + \frac{r_0^2\omega}{r} = 0$$

$$-V_0\left(1-\frac{r_0^2}{r^2}\right)\cos\theta = 0 \Rightarrow r = r_0$$

1. If $r_0\omega < 2V_0$, there are two stagnation points on the cylinder.

$$S_1\left(r = r_0, \theta = -\sin^{-1}\left(\frac{r_0\omega}{2V_0}\right)\right)$$

$$S_2\left(r = r_0, \theta = \pi - \sin^{-1}\left(\frac{r_0\omega}{2V_0}\right)\right)$$

2. If $r_0\omega = 2V_0$, there is one stagnation point on the cylinder.

$$S\left(r = r_0, \theta = -\frac{\pi}{2}\right)$$

3. If $r_0\omega > 2V_0$, there is one stagnation point away from the cylinder surface.

$$S\left(r = \frac{r_0^2\omega + \sqrt{r_0^4\omega^2 - 4V_0^2r_0^2}}{2V_0^2}, \theta = -\frac{\pi}{2}\right)$$

The other value of r is $r = \frac{r_0^2\omega - \sqrt{r_0^4\omega^2 - 4V_0^2r_0^2}}{2V_0^2}$ which is less than $r_0$ and is not acceptable.

4. If $V_0 = 0$, there is no stagnation point.

Equation of equipotental lines is obtained as followings [1,12,13]

$$\phi(r,\theta) = -V_0\left(r+\frac{r_0^2}{r}\right)\cos\theta + r_0^2\omega\theta = c \Rightarrow$$

$$-V_0(x^2+y^2+r_0^2)x + r_0^2(x^2+y^2)\times$$
$$\omega\tan^{-1}\left(\frac{y}{x}\right) = c(x^2+y^2) \qquad (10)$$

Equation of stream lines is as below [1,12,13]

$$\varphi(r,\theta) = -V_0\left(r-\frac{r_0^2}{r}\right)\sin\theta - r_0^2\omega\ln r = c \Rightarrow$$

$$-V_0(x^2+y^2-r_0^2)y - \frac{1}{2}r_0^2(x^2+y^2)\times$$
$$\omega\ln(x^2+y^2) = c(x^2+y^2) \qquad (11)$$

According to the Bernoulli equation, pressure distribution over the cylinder is as followings [1,12,13]

$$p = p_0 + \frac{1}{2}\rho(V_0^2 - V^2) = p_0 + \frac{1}{2}\rho \times \left[V_0^2(1 - 4\sin^2\theta) - 4V_0 r_0 \omega \sin\theta - r_0^2\omega^2\right]$$

Pressure coefficient is defined as [1,12,13]

$$c_p = \frac{p - p_0}{\frac{1}{2}\rho V_0^2} \Rightarrow$$

$$c_p = 1 - 4\sin^2\theta - 4\left(\frac{r_0\omega}{V_0}\right)\sin\theta - \left(\frac{r_0\omega}{V_0}\right)^2$$

Drag force is defined as the component of resultant force in the opposite direction of the free stream [1,12,13].

$$D = \int_0^{2\pi} p\cos\theta r_0 d\theta \Rightarrow$$

$$D = 0 \qquad (12)$$

Lift force is defined as the component of resultant force normal to the free stream direction [1,12,13].

$$L = \int_0^{2\pi} p\sin\theta r_0 d\theta \Rightarrow$$

$$L = 2\pi\rho V_0 r_0^2 \omega \qquad (13)$$

Circulation is defined as [1,12,13]

$$\Gamma = \oint_c u_\theta ds = \int_0^{2\pi} u_\theta r_0 d\theta \Rightarrow$$

$$\Gamma = 2\pi r_0^2 \omega \qquad (14)$$

From Equations 13 and 14 lift force can be written as:

$$L = \rho V_0 \Gamma \qquad (15)$$

This equation that relates lift force to the circulation is known as the Kutta-Joukowski theorem [1,12,13].

## 4. VALIDATION OF THE ANALYTICAL MODEL WITH THE CFD ANALYSIS

For validation of the analytical solution, a CFD code was established to solve the flow flied. Boundary conditions for numerical solution are as $p_0 = 0, \omega = 0, V_0 = 10\text{m/s}, \rho = 1.225\text{kg/m}^3, r_0 = 0.05\text{m}$ Free stream Reynolds number ($Re_D = \rho V_0 D/\mu$) is $3.42\times10^4 < 5 \times 10^5$ and consequently flow over the cylinder is laminar [1]. Computational domain for CFD solution is depicted in Figure 2. By solving Navier-Stokes equations, static pressure distribution was obtained [17,18].

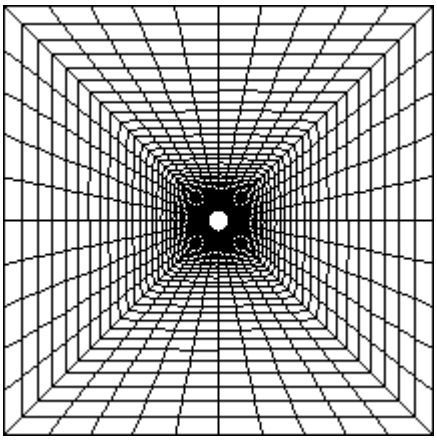

**Figure 2.** Computational domain over the cylinder

The computed values of the pressure coefficient over the cylinder are given in Table 1.
Comparison of numerical and analytical pressure coefficients is shown in Figure 3. It is observed that behind the cylinder, flow is separated at $\theta = 151.87°$. For $\theta < 90°$, there is a good agreement between the computed and the analytical $c_p$.

**TABLE 1. Computed pressure coefficient by the CFD technique**

| x(m) | $c_p$ | x(m) | $c_p$ | x(m) | $c_p$ |
|---|---|---|---|---|---|
| -0.0500 | -0.088 | -0.0226 | -1.474 | 0.0293 | -1.460 |
| -0.0496 | -0.131 | -0.0190 | -1.798 | 0.0323 | -1.161 |
| -0.0493 | -0.171 | -0.0154 | -2.056 | 0.0353 | -0.877 |
| -0.0484 | -0.191 | -0.0116 | -2.284 | 0.0379 | -0.585 |
| -0.0475 | -0.186 | -0.0078 | -2.446 | 0.0404 | -0.308 |
| -0.0460 | -0.170 | -0.0039 | -2.573 | 0.0425 | -0.029 |
| -0.0445 | -0.156 | 0.0000 | -2.632 | 0.0445 | 0.215 |
| -0.0425 | -0.1498 | 0.0039 | -2.643 | 0.0460 | 0.450 |
| -0.0404 | -0.147 | 0.0078 | -2.598 | 0.0475 | 0.639 |
| -0.0379 | -0.172 | 0.0116 | -2.504 | 0.0484 | 0.801 |
| -0.0353 | -0.262 | 0.0154 | -2.370 | 0.0493 | 0.910 |
| -0.0323 | -0.485 | 0.0190 | -2.184 | 0.0496 | 0.981 |
| -0.0293 | -0.786 | 0.0226 | -1.977 | 0.0500 | 1.003 |
| -0.0260 | -1.151 | 0.0260 | -1.717 | | |

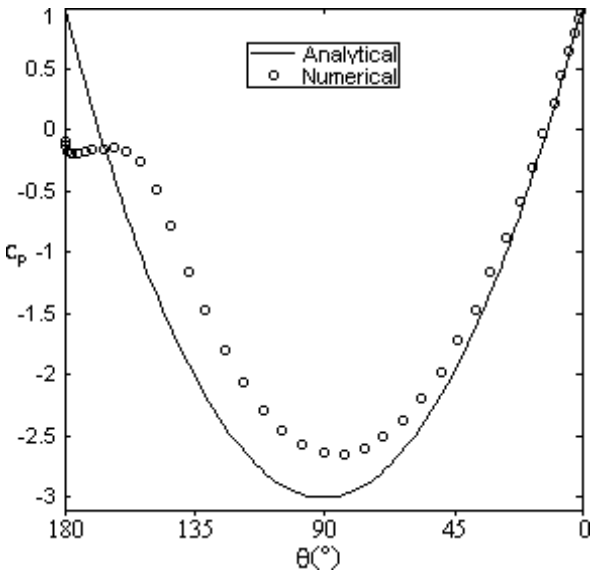


**Figure 3.** Comparison of numerical and analytical pressure coefficient for $p_0 = 0$, $\omega = 0$, $V_0 = 10$ m/s, $\rho = 1.225$ kg/m$^3$, $r_0 = 0.05$ m

Because of adverse pressure gradient at $\theta > 90°$, discrepancies between the CFD results and the analytical equation increases and after separation point, the analytical formula fails to be matched with the computed data.

## 5. RESULTS AND DISCUSSIONS

Lift force of the cylinder versus rotational speed and radius is depicted in Figure 4. At negative rotational speeds, because free stream and rotational speeds are in the opposite directions at the upper surface and in the same direction at the bottom surface, lift force decreases. Higher radius of the cylinder is tantamount to higher induced speed due to rotation that increases absolute value of the lift force at constant rotational speed.

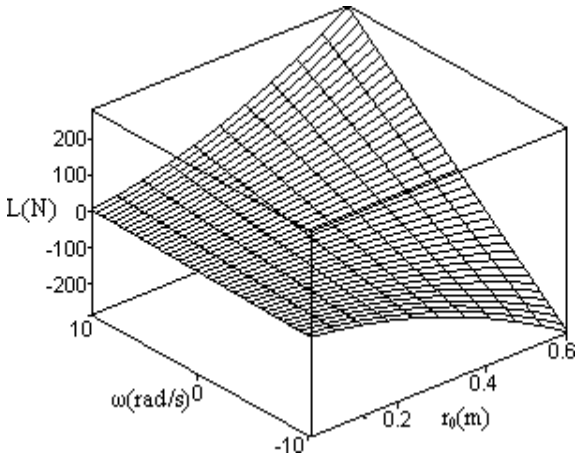


**Figure 4.** Lift force versus $r_0$ and $\omega$ at $V_0 = 10$ m/s

Lift force is shown Figure 5 at various rotational and free stream velocities. It is perceived that when both $\omega$ and $V_0$ are negative or positive, the maximum lift is obtained.

The streamlines over the cylinder are shown in Figure 6 at various rotational speeds. This figure has four parts as followings

(a) $\omega = 0$ and $r_0\omega < 2V_0$, there are two stagnation points, one at $\theta = 0$ and the other at $\theta = \pi$.

(b) $r_0\omega < 2V_0$, there are two stagnation points.

(c) $r_0\omega = 2V_0$, there is one stagnation point at $\theta = -\pi/2$.

(d) $r_0\omega > 2V_0$, there is one detached stagnation point at $\theta = -\pi/2$.

As depicted in this figure, for $\omega = 0$, stagnation points lay on the cylinder surface at $\theta = 0, \pi$,

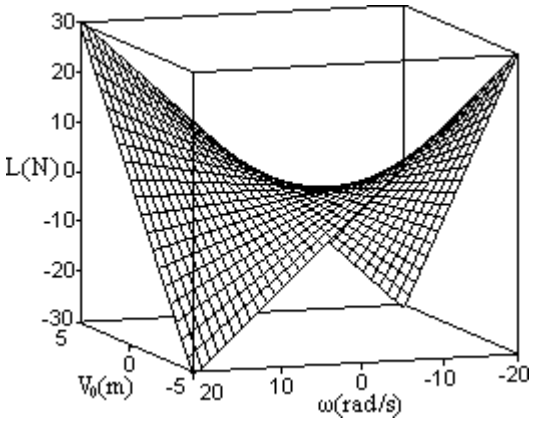


**Figure 5.** Lift force versus $V_0$ and $\omega$ at $r_0 = 0.2$ m

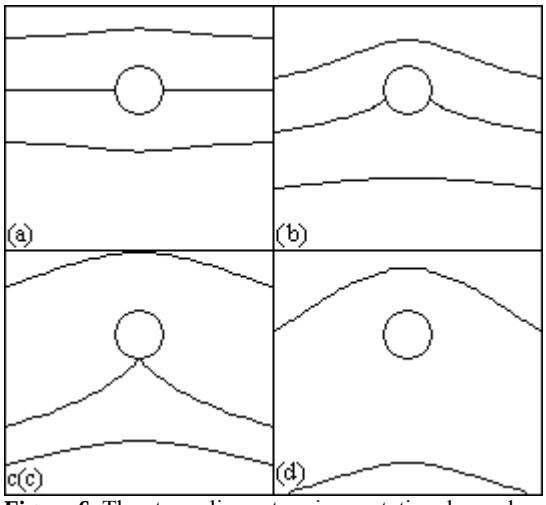


**Figure 6.** The streamlines at various rotational speeds for $V_0 = 10$ m/s, $r_0 = 1$ m, (a) $\omega = 0$ rad/s, (b) $\omega = 10$ rad/s, (c) $\omega = 20$ rad/s and (d) $\omega = 30$ rad/s

however, by increasing rotational speed, they move downward and finally when $r_0\omega$ is going to be greater than $2V_0$, they leave the cylinder surface at $\theta = -\pi/2$.

The streamlines over the cylinder are depicted in Figure 7 at various free stream velocities.

(a) $V_0 = 0$, there is no stagnation point.

(b) $r_0\omega > 2V_0$, there is one detached stagnation point at $\theta = -\pi/2$.

(c) $r_0\omega < 2V_0$, there are two stagnation points.

(d) $r_0\omega < 2V_0$, there are two stagnation points.

As illustrated in this figure, when $V_0 = 0$, there is no stagnation point. By increasing free stream velocity, one detached stagnation point forms far from the cylinder surface at $\theta = -\pi/2$ and as free stream speed increases, this point moves toward the cylinder and finally lay on its surface at $\theta = -\pi/2$. By further enhancement of $V_0$, two stagnation points appear on the cylinder surface.

The streamlines at high free stream and rotational speeds are shown in Figure 8. At high free stream velocity, flow is similar to the case in which rotational speed is zero and there are two stagnation points at $\theta = 0, \pi$. At high rotational speed, flow is similar to the case in which free stream velocity is zero and there is no stagnation point.

Variation of the pressure coefficient at various rotational speeds is illustrated in Figure 9. It is perceived that at upper wall of the cylinder,

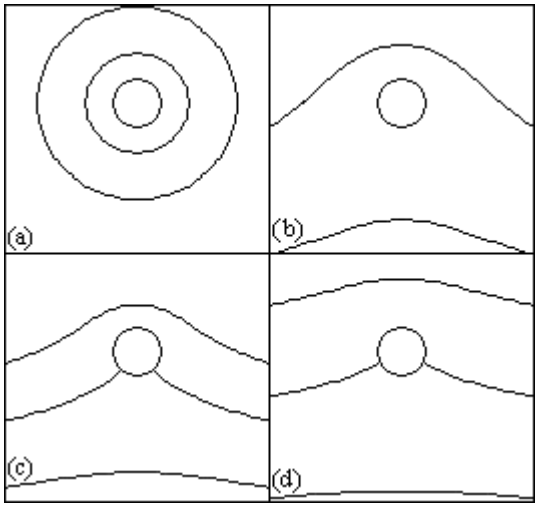


**Figure 7.** The streamlines at various free stream velocities for $\omega = 15$ rad/s, $r_0 = 1$ m, (a) $V_0 = 0$ m/s, (b) $V_0 = 5$ m/s, (c) $V_0 = 10$ m/s and (d) $V_0 = 15$ m/s

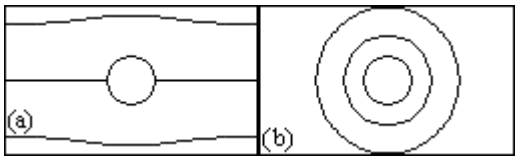


**Figure 8.** The streamlines over the cylinder at high free stream and rotational velocities for $r_0 = 1$ m, (a) $\omega = 15$ rad/s, $V_0 = 1000$ m/s, (b) $\omega = 4000$ rad/s, $V_0 = 10$ m/s

pressure coefficient decreases with the rotational velocity and on the bottom wall increases that causes higher lift force at high rotational velocities as shown in Figures 4 and 5. Symmetric distribution of the pressure coefficient demonstrates that drag force should be zero as obtained in Equation 12. However, pressure distribution is not symmetric in realty and drag force would not be zero as depicted in Figure 3.

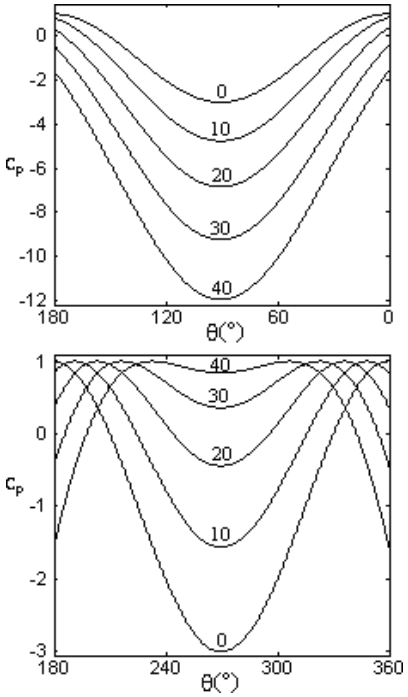


**Figure 9.** Pressure coefficient distribution at various rotational velocities for $\rho = 1.225$ kg/m$^3$, $V_0 = 5$ m/s, $r_0 = 0.2$ m (Numbers written on the figure denote rotational speed in rad/s.)

Pressure coefficient at various radii of the cylinder is shown in Figure 10. It is observed that on the upper wall, pressure coefficient decreases as radius increases. However, at the bottom wall, changes of the pressure depended on the interaction of the free steam and rotational velocities. At low radii, difference of $V_0$ and $r_0\omega$ is low which is equivalent to high pressure coefficient and at higher radii, this difference is greater and causes lower pressure coefficient.

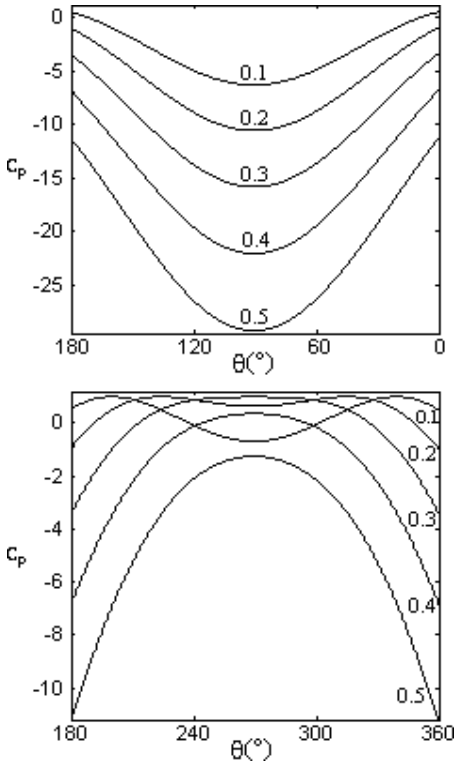


**Figure 10.** Pressure coefficient distribution at various radii for $\omega = 35$ rad/s, $V_0 = 5$ m/s, $\rho = 1.225$ kg/m$^3$ (Numbers written on the figure denote radius of the cylinder in m)

## 6. CONCLUSIONS

Flow over stationary and rotating cylinders was investigated by direct solution of the Laplace equation and numerical solution. Results of the mathematical solution were exactly identical to the singularity method. Because of dealing with real physical parameters, this solution is more perceptible and tangible than conventional singularity technique. For verifying accuracy of the mathematical analysis, a CFD code was established to solve the flow field over the cylinder using the Finite Volume Method (FVM). The proposed analytical model was in good agreement with the numerical simulation before the separation point. Velocity potential and stream functions of the flow were derived from the solution of the Laplace equation and equipotential and stream lines were obtained from these functions,

respectively. Stagnation points for various free stream conditions, cylinder radius and rotational speed were located and discussed. Drag and lift forces and circulation were calculated that were the same as the singularity technique.

## 7. REFERENCES


1. Shames, I. H., "Mechanics of fluids", Mc Graw-Hill, (1982).
2. Robinson, T., "Revolution in the air", ***Aerospace International***, (November 2004), 20-23.
3. Duddempudi, D., Yao, Y. and Edmondson, D., "CFD Investigation of Flow over a Generic Fanwing Airfoil", ***43rd AIAA Aerospace Sciences Meeting and Exhibit***, Reno, Nevada (2005).
4. Duddempudi, D., Yao, Y., Edmondson, D., Yao, J. and Curley, A., "Computational study of flow over generic fan-wing airfoil", ***Aircraft Engineering and Aerospace Technology***, Vol. 79, No. 3, (2007), 238–244.
5. Thong, Q. D., Bushnell, P. R., (2009), "Aerodynamics of cross-flow fans and their application to aircraft propulsion and flow control", ***Progress in Aerospace Sciences***, Vol. 45, (2009), 1-29.
6. Askari, S. and Shojaeefard, M. H., "Numerical simulation of flow over an airfoil with a cross flow fan as a lift generating member in a new aircraft model", ***Aircraft Engineering and Aerospace Technology***, Vol. 81, No. 1, (2009), 56–64.
7. Askari, S. and Shojaeefard, M. H., "Shape optimization of the airfoil comprising a cross flow fan", ***Aircraft Engineering and Aerospace Technology***, Vol. 81, No. 5, (2009), 407–415.
8. Mirzaee, B., Khoshravan, E. and Razavi, S. E., "Finite-volume solution of a cylinder in cross flow with heat transfer", ***International Journal of Engineering, Transaction A***, Vol. 15, No. 3, (2002), 303-314.
9. Lopez, J. M., Hart, J. E., Marques, F., Kittelman, S. and Shen, J., "Instability and mode interactions in a differentially driven rotating cylinder", ***Journal of Fluid Mechanics***, Vol. 462, (2002), 383-409.
10. Rahimi, A. B., "Pressure calculation in the flow between two rotating eccentric cylinders at high Reynolds numbers", ***International Journal of Engineering***, Vol. 9, No. 4, (1996), 201-209.
11. Heidarinejad, G. and Delfani, S., "Direct numerical simulation of the wake flow behind a cylinder using random vortex method in medium to high Reynolds numbers", ***International Journal of Engineering***, Vol. 13, No. 3, (2000), 33-50.
12. Katz, J. and Plokin, A., "Low-Speed Aerodynamics: From Wing Theory to Panel Methods", McGraw-Hill, (1991).
13. Anderson, D., "Fundamentals of Aerodynamics", McGraw-Hill, (1991).
14. Asmar, N. H., "Partial Differential Equations with Fourier series and Boundary Value Problems", Prentice Hall, (2000).
15. Kreyszig, E., "Advanced Engineering Mathematics", John Wiley & Sons, (1999).
16. Simmons, G. F., "Differential Equations with Applications and Historical Notes", McGraw-Hill, (1991).
17. Versteeg, H. K. and Malalasekera, W., "An introduction to computational fluid dynamics: the finite volume method", Harlow: Longman, (1995).
18. Patankar, S., "Numerical heat transfer and fluid flow", McGraw-Hill, (1980).